

Cell Reports, Volume 16

Supplemental Information

**An Integrative Analysis of the InR/PI3K/Akt
Network Identifies the Dynamic Response
to Insulin Signaling**

Arunachalam Vinayagam, Meghana M. Kulkarni, Richelle Sopko, Xiaoyun Sun, Yanhui Hu, Ankita Nand, Christians Villalta, Ahmadali Moghimi, Xuemei Yang, Stephanie E. Mohr, Pengyu Hong, John M. Asara, and Norbert Perrimon

Content

- Experimental Procedures
- Tables S1 to S6
- Figures S1 to S5
- References

Experimental Procedures

Tandem affinity purification

Tandem affinity purification was performed as previously described (Friedman et al., 2011; Kwon et al., 2013). Briefly, InR, chico, Pi3K92E, Pi3K21B, Pten, Pdk1, Akt1, Ikb1, Tsc1, gig, Rheb, rictor, S6k, S6kII, dm, foxo, Thor, B4, melt and sima were used as bait proteins. Baits were sub-cloned into the pMK33-CTAP vector for inducible expression of TAP-tagged bait proteins. S2R+ cells were transfected with the pMK33-CTAP constructs to generate stable cell lines. Bait expression was induced by overnight incubation in the presence of CuSO₄ and cells were either lysed directly or induced with 25 mg/mL Insulin for 10 or 30 minutes and then lysed. TAP experiments for each bait condition were performed as three independent replicates. The complexes were digested with trypsin overnight at pH=8.3, the digest stopped with 5% trifluoroacetic acid (TFA), the peptides purified using C18 Zip Tip (Millipore) and eluted in 10 µL of LC-MS/MS A buffer (0.1% formic acid). 5-µL aliquot was injected onto the microcapillary LC-MS/MS system via data dependent acquisition (DDA) on a Thermo Orbitrap XL and Thermo Orbitrap Elite via collision induced dissociation (CID) as described in Friedman et al. (2011). Typically, between 3,000 and 6,000 MS/MS spectra were collected per run. All LC-MS/MS runs were separated by at least one blank run to prevent column carryover. Raw MS/MS spectra are available upon request. All collected MS/MS fragmentation spectra were searched against a dmel-all-translation protein database (FlyBase Consortium) using the Sequest search engine in Proteomics Browser Software (Thermo Scientific) as previously described (Friedman et al., 2011; Kwon et al., 2013). An FDR rate of 1.5% for peptide hits and 1.7% for protein hits was calculated on the basis of the number of reversed database hits above the scoring thresholds.

Statistical Analysis of Tandem affinity purification data

The SAINT algorithm was used to calculate the probability scores for the interaction between bait and prey observed by MS. SAINT assigns a probability value for each bait-prey relationship based on the spectral count distribution. To model the spectral count distribution of the non-specific interactions, we performed 21 independent control AP-MS experiments (using an empty vector as bait). SAINT was downloaded from <http://saint->

apms.sourceforge.net/Main.html and implemented locally. The program was run with control IPs option and using default parameters. We ran the algorithm separately for each condition and computed the probability that the interaction was true in any condition. To determine a high-confidence threshold, we created a positive reference set (PRS) from the literature and a random reference set (RRS) for non-specific interactions as described in Kwon et al. (Kwon et al., 2013). Briefly, PRS consist of literature curated PPIs that overlaps with InsulinNet pull-down data. To construct RRS, we first compiled a list of non-specific interactors by analyzing raw DPiM dataset, which is a large-scale AP/MS dataset in Drosophila. Non-specific interactors were defined as proteins that pulldown with approximately 1000 experiments in raw DPiM dataset. From this non-specific interactor list, we randomly sampled 1000 RRS sets consisting of interactions between baits and non-specific interactors, existing in the unfiltered InsulinNet (size of each RRS is equal to the size of PRS). Both PRS and RRS datasets are provided in Table S1. We used PRS and RRS to access the true positive rate (specificity) and false positive rate (1 – specificity) of SAINT score at various cutoff values. We selected SAINT score cutoff 0.95 because at this cutoff we achieved 4% or less false positive rate (at Baseline, 10 min and 30 min networks). Note that the true positive rates are variable at this cutoff (maximum of 60% for Baseline network and minimum of 45% for 30 min network).

We used Jaccard index to compute the similarity between the baits based on shared prey proteins. Similarity between bait a and b is computed as:

$$J(a, b) = \frac{(A \cap B)}{(A \cup B)}$$

where A is the set of prey proteins interacts with bait a and B is prey proteins interact with bait b. Next, we clustered the bait proteins based on similarity using hierarchical clustering. Clustering and visualizations are performed using “heatmap” function from R (<https://www.r-project.org/>).

Web interface for the InsulinNet-PPI

We built an interactive, dynamic web interface for InsulinNet

(<http://fgrtools.hms.harvard.edu/InsulinNetwork/>) using Cytoscape javascript library (Lopes et al., 2010) and JAVA. InsulinNet visualization (layout) was created using Cytoscape (Shannon et al., 2003) and the corresponding JSON files were exported. These JSON files were used as an input to cytoscape.js and visualized at InsulinNet dynamic web page. Note, display layout of network and the style such as node color, shape and edge colors were predefined at the Cytoscape JSON files. The search box given in the user interface allows the user to search a particular protein in the network based on gene ID or gene symbol. In response to the user search a sub-network gets generated dynamically using the query gene and its interacting partners. Also the sub-network gets displayed using a new layout.

RNAi screens

RNAi screening was performed to validate novel components of InsulinNet-PPI as described previously (Friedman and Perrimon, 2006; Friedman et al., 2011; Kockel et al., 2010). Briefly, S2R+ cells were seeded in microplates containing dsRNAs targeting genes of interest for 72hrs. Cells were stimulated with insulin for 10 or 30 minutes (or not stimulated with insulin for baseline condition), fixed and stained for Akt and ERK activity using In-Cell Western (ICW) Assay. Monoclonal pAkt (Ser505) and pERK (Thr202/Tyr204) antibodies from Cell Signaling technologies were used to quantify the Akt and ERK activities at 700 nm (I_{700}). Total protein stain with IRDye 800 CW (N-hydroxysuccinimidyl ester (NHS) reactive dye) (I_{800}) was used for cell number normalization. Corrected phospho-antibody signal was calculated as I_{700}/I_{800} . The screens were performed in triplicate. To define a hit, we computed \log_2 fold-change value of the phospho-antibody signal of a gene compared to the control as described previously (Friedman and Perrimon, 2006; Friedman et al., 2011; Kockel et al., 2010). Genes with \log_2 fold-change ≥ 0.5 are defined as negative regulators and ≤ -0.5 is defined as positive regulators.

Phosphoproteomic analyses

Cells were grown as above for AP-MS experiments: lysed either directly or induced with 25 µg/ml insulin for 10 or 30 minutes and then lysed on ice in 8 M urea, 75 mM NaCl, 50 mM Tris, pH 8.2, protease inhibitors cocktail (Roche), 1 mM NaF, 1 mM β-glycerophosphate, 1 mM sodium orthovanadate, 10 mM sodium pyrophosphate, 1 mM PMSF. Lysates were stored at -80°C until further processing essentially as previously described (Sopko et al., 2014). Briefly, one milligram of protein from each replicate was reduced, alkylated, and digested with trypsin. TMT labeling was as follows: untreated - TMT126; TMT127; 10 minutes insulin - TMT128; TMT129; 30 minutes insulin - TMT130; TMT131. Twelve chromatography fractions from strong cation exchange (SCX) were subjected to phosphopeptide enrichment using IMAC-Select Affinity Gel (Sigma-Aldrich) and subsequent peptide desalting with Stagetips. Samples were analyzed on an LTQ OrbiTrap Velos mass spectrometer (Thermo Fisher Scientific) using a data-dependent Top10-MS2 method using (higher-energy collisional dissociation) HCD for reporter ion quantitation. Peptide identification and filtering, and data normalization and phosphosite localization was performed as previously described (Sopko et al., 2014).

Statistical Enrichment analysis

Motif enrichment analysis: We used the online MotifX program (<http://motif-x.med.harvard.edu/>) to identify enriched kinase consensus motifs (Chou and Schwartz, 2011). Dynamic phosphosites from each dynamic class were analyzed separately. To identify motifs, we used 13 amino acid peptide sequences centered on the phosphosite (6 amino acids upstream and downstream of the phosphosite) as input, all the *Drosophila* protein sequences as background, and motifs with occurrences ≥ 3 and P-value ≤ 0.001 were selected as enriched motifs.

Predicting kinase-substrate relationships: We used NetPhorest to predict kinase-substrate relationships (Miller et al., 2008). For a given phosphosite, the tool predicts one or more kinases as upstream regulators based on the linear motif atlas. NetPhorest program was

downloaded from <http://www.netphorest.info/> and locally installed. To identify the kinase consensus motifs we run the NetPhorest program with the default parameters. Note, we used all the prediction analysis without using any score cutoff.

Comparative network analysis

To compare the InsulinNet-PPI with literature-based interactions, we compiled the *Drosophila* PPIs from public database such as BioGrid (Stark et al., 2011), IntAct (Kerrien et al., 2012), MINT (Licata et al., 2012) and DIP (Salwinski et al., 2004). Further, a *Drosophila* interologs network was constructed by predicting PPIs based on experimentally identified PPIs from human, mouse, zebrafish, *C. elegans* and *S. cerevisiae*. The interolog networks were compiled from BioGrid, IntAct, MINT, DIP, HPRD (Keshava Prasad et al., 2009) and DroID (Murali et al., 2011) databases. Kinase-substrate was constructed using NetPhorest program using experimentally verified phosphorylation sites as input. Domain-domain interaction (DDI) network was compiled from DOMINE database (Yellaboina et al., 2011), which includes DDIs inferred from PDB entries, and those that are predicted by 13 different computational approaches. Note, we only considered high-confidence DDIs and those derived from crystal structures for the analysis. *Drosophila* genetic interactions were compiled from FlyBase (<http://flybase.org/>), BioGrid and DroID databases. All these datasets are downloaded from the corresponding source databases and the gene/protein identifiers were mapped to FlyBase gene identifiers. PPIs from other species were mapped to *Drosophila* using the ortholog annotation from DIOPT (Hu et al., 2011).

To estimate the significance of overlap between the InsulinNet-PPI and other literature network, we created random networks with same size and degree distribution as InsulinNet-PPI (sampled from all expressed genes in S2R+ cells) and computed the random expected overlap. Mean and standard deviation of random distribution is computed from 1,000 simulations of random networks. Z-scores and P-values were computed by comparing the observed overlap with random distribution (modeled as Gaussian distribution). Note, similar approach is used to compare gene/protein list, where the observed overlap is compared with random distribution sampled from S2R+ expressed genes.

Gene Ontology enrichment analysis

We performed GO enrichment analysis using a java program developed in-house, which is adapted from GO::TermFinder tool (Boyle et al., 2004). GO annotations were downloaded from NCBI *Drosophila* gene2go (ftp.ncbi.nlm.nih.gov/gene/DATA/gene2go.gz). Enrichment P-values were calculated using cumulative hypergeometric probabilities based on the overlap between the input list and gene set annotated with specific GO term, the size of gene set, the size of hit list and background (list of all protein coding genes).

Protein complex enrichment analysis

We applied COMPLETEAT tools to identify enriched protein complexes in the InsulinNet. COMPLETEAT uses comprehensive *Drosophila* protein complex resources that are compiled either from literature curation or predicted from PPI networks. Since COMPLETEAT analysis is designed to analyze raw dataset and to define the cutoff at the level of protein complexes, we used unfiltered PPI networks from all three time points as input. For a given prey protein P_i that interact with bait B_j we computed a modified spectral count value (M_{ij}) as follows:

$$M_{ij} = (SC_{ij} \times S_{ij})$$

Where SC_{ij} is spectral count value of the prey P_i that interacts with bait B_j . S_{ij} is SAINT score of the prey P_i that interacts with bait B_j .

We also computed N_{ij} (normalized M_{ij}), where the M_{ij} of stimulus condition (10 or 30 minutes data) is normalized with the M_{ij} of baseline as follows

$$N_{ij} = \frac{M_{ij} \text{ Stimulus}}{M_{ij} \text{ Baseline}}$$

In case of prey P_i that interacts with multiple baits, we used the maximum value of M_{ij} or N_{ij} that corresponds to maximum $|N_{ij}|$. The tool maps the M_{ij} or N_{ij} values of individual protein to the complexes and then the complex score is calculated by computing the interquartile mean.

Furthermore, a P-value is computed to estimate the significance of complex scores as compared to 1000 random-complexes of the same size. We also removed redundant complexes using COMPLEAT non-redundant function.

To identify stably associated complexes M_{ij} was used as input. PPIs from all the three networks are analyzed separately and complexes identified as significant in all the three time points (P-value ≤ 0.001 and complex score ≥ 1) were selected as stably associated complexes. To identify dynamic complexes N_{ij} was used as input. Networks from 10 minutes and 30 minutes are analyzed separately. Complex is defined “associating” if P-value is ≤ 0.001 and complex score ≥ 1 . Similarly, a complex is defined “dissociating” if the P-value is ≤ 0.001 and complex score ≤ -1 . Next, we selected complexes that are anchored with at least one high-confidence interaction for further analysis.

Signpredictor tool was used to predict edge signs between the protein complexes and the insulin pathway. To construct the phenotype matrix we used 6 RNAi screens from InsulinNet-RNAi dataset and 49 published RNAi screens that are described in Vinayagam et al. (2014). Interactions with ≥ 2 matching phenotypes are considered for prediction and sign score cutoff of ≥ 1 and ≤ -1 were used to predict positive and negative signs, respectively. Note that for sign prediction we only considered the PPIs from InsulinNet-PPI that connect the enriched complexes and the core components of the pathway. In case of more than one interaction between the protein complex and the core components, we manually inspected those cases and assigned the sign that is more frequent. Note that the sign predicted between a complex member and the negative regulators, such as PTEN, TSC1/TSC2, are treated differently. For instance, a positive interaction with PTEN is considered as a negative sign with respect to pathway outcome.

Co-immunoprecipitation and Western blotting

Co-immunoprecipitation and Western blotting were performed as described before (Vinayagam et al., 2013). Briefly, an expression construct for a FLAG and HA double-tagged bait protein was co-transfected with either a MYC-tagged prey construct or MYC-tagged GFP as a control in S2R+

cells. Subsequently, the cells were treated with copper sulfate to induce expression of the tagged proteins. Cells were untreated or stimulated with insulin for 10 and 30 minutes and the cell lysates were prepared and subjected to immunoprecipitation using anti-FLAG M2 Affinity Gel (Sigma). Immunoprecipitates were resolved by SDS-PAGE and probed with anti-Myc Tag (EMD Millipore 05-724) or anti-HA (Roche 11867423001) antibodies. For Infrared imaging-based Western blot analysis, membranes were probed with anti-phospho-S6k (Cell Signaling Technology # 9209) and anti-tubulin (Sigma T5168) antibodies. Alexa-Fluor 680 goat anti-rabbit (Life Technologies) and donkey anti-mouse IRDye 800CW (LI-COR Biosciences 926-32212) secondary antibodies were used for detection with a LI-COR Odyssey system.

Quantitative real-time RT-PCR

Drosophila S2R+ cells were treated with DMSO, LY294002, Rapamycin for 1 hour before stimulating with Insulin for 6 hours. For RNAi experiments Drosophila S2R+ cells were treated with long dsRNA targeting reptin and pontin for 72 hours prior to stimulating with Insulin for 6 hours. After 6 hour stimulation with Insulin total RNA was extracted using Trizol following the manufacturers protocol and cleaned up using Qiagen's RNeasy kit. SYBR green real-time qPCR was performed using the following primer pairs:

b-tubulin (Forward) AGTTCACCGCTATGTTCA

b-tubulin (Reverse) CGCAAACATTGATCGAG

rRNA (Forward) CCCAAAGGCAAATATTGAA

rRNA (Reverse) TAATGAGCCTTTTGCGGTTT

Fly stocks and phenotypic analyses. Dmef2-Gal4 drives transgene expression in all body wall muscles. For transgene expression with the Gal4-UAS system, flies were reared at 25°C. Hairpin lines were obtained from TRiP facility at Harvard Medical School (<http://www.flyrnai.org/TRiP->

HOME.html). Histology, laser-scanning confocal microscopy and image analysis, as well as staining reagents are described in details in (Vinayagam et al., 2013). Muscles VL3 and VL4 of abdominal segments 2-5 from wandering third instar larvae were stained with DAPI (4',6-diamidino-2-phenylindole, 1 µg/ml) to visualize nuclei, Alexa633-conjugated phalloidin (1:100) for F-actin, and anti-Fibrillarin antibody [EnCore Biotechnology #MCA-38F3(47) at (1:100)] followed with Alexa555-conjugated secondary antibodies (Molecular Probes) for nucleoli.

Supplementary Tables

Table S1 (related to Figure 2): Datasets corresponding to InsulinNet-PPI.

Bait proteins: List of 20 canonical components used as bait proteins.

Raw data: PPIs from TAP-MS data without filtering non-specific interactions.

Canonical interactions: List of canonical interactions identified in unfiltered network and the corresponding SAINT scores.

InsulinNet-PPI: List of high confidence PPIs (InsulinNet-PPI) identified with SAINT score cutoff ≥ 0.95 .

Literature overlap: List of InsulinNet-PPIs supported by other literature evidences and/or predicted interactions (see Experimental Procedures)

Relevant overlap: List of overlapping PPIs between InsulinNet-PPI and other relevant networks such as MAPK (Friedman et al., 2011), DPiM (Guruharsha et al., 2011) and Glatter et al (Glatter et al., 2011). These networks were compiled from the supplementary materials of the corresponding publications.

Enrichment: Enrichment analysis of overlap between InsulinNet-PPI with other relevant networks. To compute the expected overlap, we generated 1000 randomized network for the common baits with same number of prey proteins as real network. Prey proteins are randomly selected from genes expressed in S2R+ cells. Overlap between randomized InsulinNet-PPI is compared to relevant network to estimate the expected overlap.

PRS: Data used to generate positive reference set. Note only PPIs with 3 or more evidences are selected for the analysis.

RRS: Data used to generate random reference set. Note RRS is randomly sampled from this list.

Table S2 (Related to Figure 2): Datasets corresponding to the prey proteins identified in InsulinNet-PPI.

Unique preys: List of 554 unique prey proteins that are part of InsulinNet-PPI. Note that this list includes bait proteins that are also identified as prey proteins.

GO enrichment: Results from GO enrichment analysis of the prey proteins. Enriched GO Biological Process category was listed along with the negative log of the p-values.

Ortholog mapping: List of human orthologs of the InsulinNet-PPI prey proteins. Orthologs were identified using DIOPT tool.

Disease enrichment: List of enriched disease category within the InsulinNet-PPI prey proteins. Enrichment analysis was performed using DIOPT-DIST dataset.

Gene expression: Gene expression values for prey proteins in S2R+ cell line and other relevant cell lines. RNA-Seq data with corresponding FPKM values are compiled from modENCODE (<http://www.modencode.org/>).

Table S3 (Related to Figure 3): Datasets corresponding to InsulinNet-RNAi

Amplicons: List of 480 genes selected for RNAi screen and its corresponding RNAi reagents

Raw data: RNAi screening results. Fold changes and amplicons information for 480 screened genes under each condition tested (pERK_0, pERK_10, pERK_30, pAkt_0, pAkt_10, pAkt_30).

Hits: List of genes selected as hits (regulates pAKT, pERK or both) based on the RNAi screens (InsulinNet-RNAi).

GO enrichment: Enriched GO Biological Process category for the hits and corresponding negative log of the p-values.

Overlap with other RNAi screens: Results from comparative analysis of InsulinNet-RNAi with other relevant RNAi screens.

MS overlap Enrichment: Data from comparative analysis of TAP-MS/MS dynamics with RNAi screens. Data corresponds to figure 3E.

Table S4 (Related to Figure 4): Datasets corresponding to InsulinNet-Phospho

Raw data: List of phosphosites identified using TMT-labeling approach. Data includes quantification of Phosphosites at each time point (baseline, 10 min and 30 min) in duplicates.

Fold changes values are computed by taking average of duplicates and comparing it with baseline condition.

Dynamic sites: List of dynamic sites identified (InsulinNet-Phospho) and the corresponding dynamic classification.

GO enrichment: Enriched biological process GO terms for proteins with dynamic phosphosites.

Enriched motifs: List of enriched consensus sequence motifs identified using MotifX program. Motif enrichment was computed for each dynamic class separately.

KS network: Predicted kinase-substrate network using NetPhorest program. For each dynamic phosphosite, Netphorest identifies the corresponding upstream kinase using linear motif atlas.

Overlap: Overlapping InsulinNet-Phospho proteins with InsulinNet-PPI and InsulinNet-RNAi.

Table S5 (Related to Figure 5): Datasets corresponding to InsulinNet (integrated InsulinNet-PPI, InsulinNet-RNAi and InsulinNet-Phospho datasets).

Table S6 (Related to Figure 6): Datasets corresponding to COMPLETEAT and SignedPPI analysis.

Stable: List of proteins complexes identified as significantly enriched in all three-time points (Baseline, 10 min and 30 min). COMPLETEAT complex ID, score and p-values corresponding all three-time points are shown.

Dynamic: List of proteins complexes identified as dynamic complexes (see Experimental Procedures).

Literature: Subset of enriched complexes that are annotated as literature-curated complexes at COMPLETEAT. This data corresponds to figure 6D.

Complex Sign: Inferred activation/inhibition relationship between the core-pathway and associated protein complexes in InsulinNet. Signs are predicted using SignPredictor tool (see Experimental Procedures).

Supplementary Figures

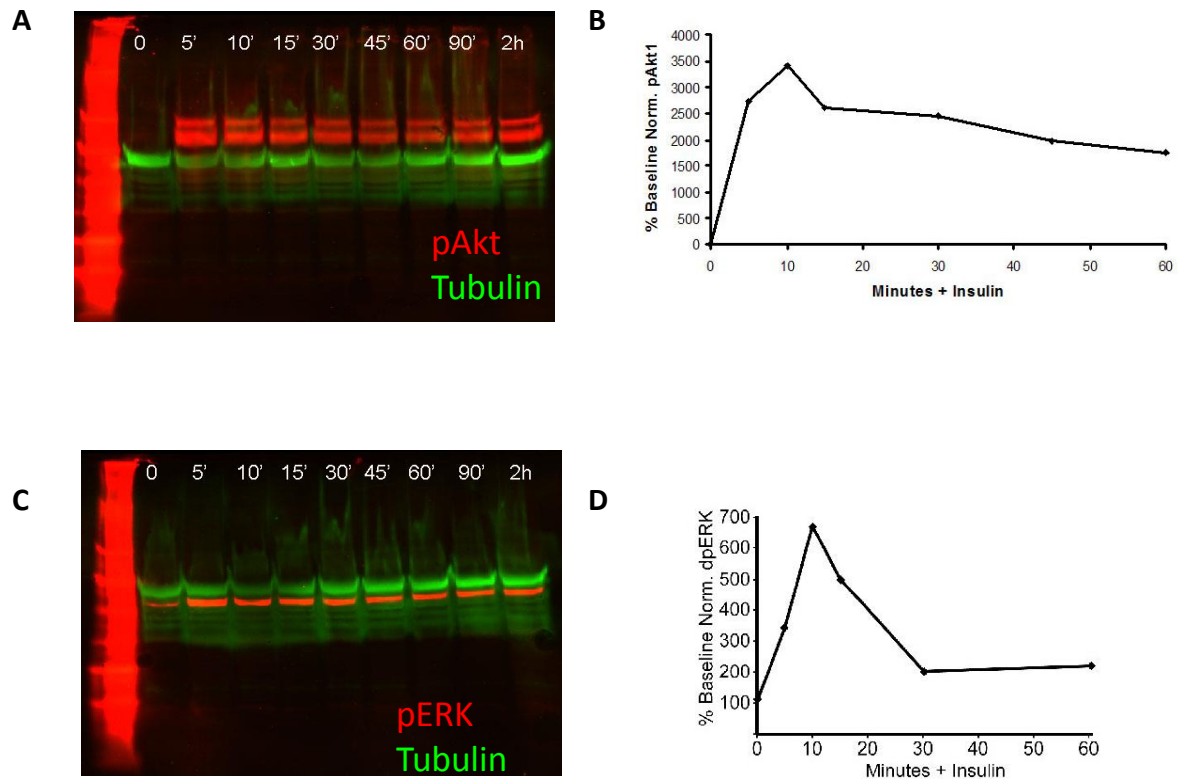


Figure S1 (Related to Figure 1): Time course of Insulin stimulation assessed by levels of phospho-Akt1 (ser 505) and dually phosphorylated ERK. **(A and B)** There is no detectable pAkt1 in S2R+ cells at baseline, and levels of pAkt1 peak at 10 minutes after induction with Insulin. pAkt1 levels drop (but stay higher than baseline) at later time points. **(C and D)** Levels of pERK also peak between 5-10 minutes after induction with Insulin and drop to near baseline levels at later time points

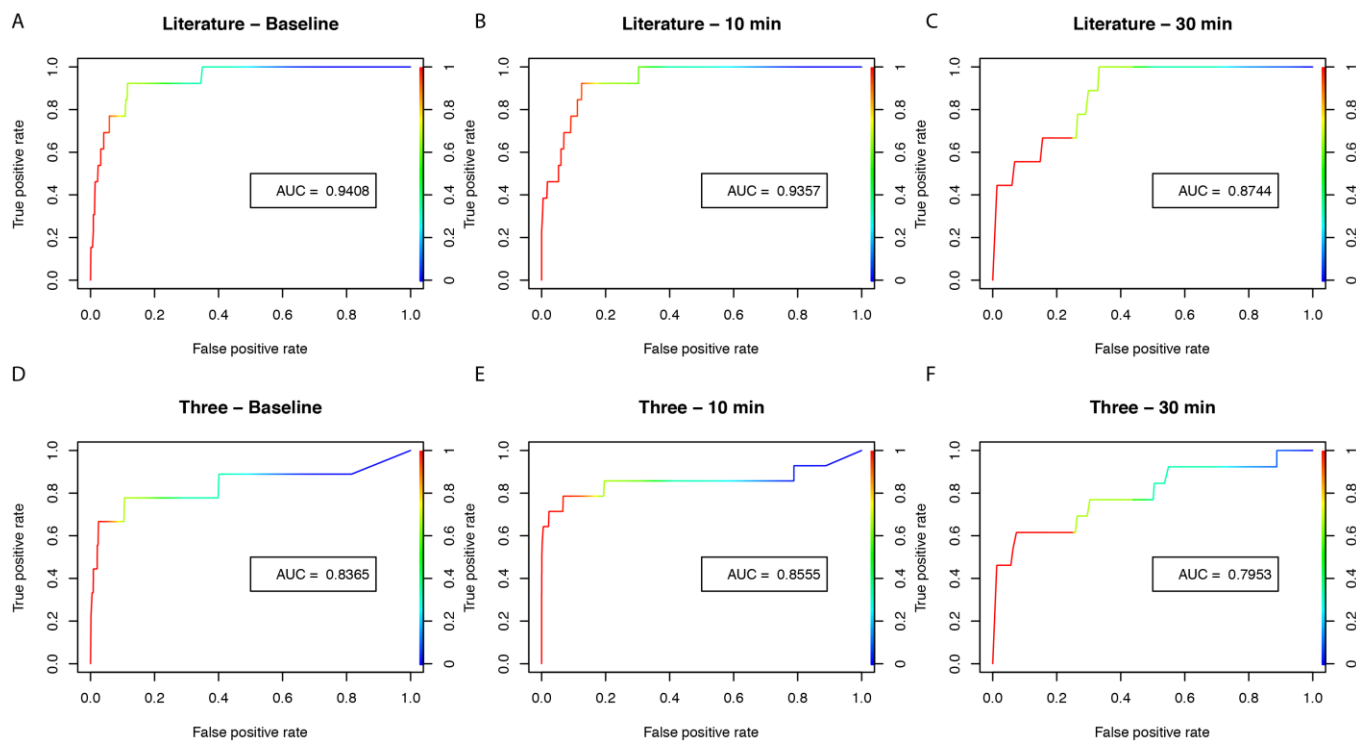
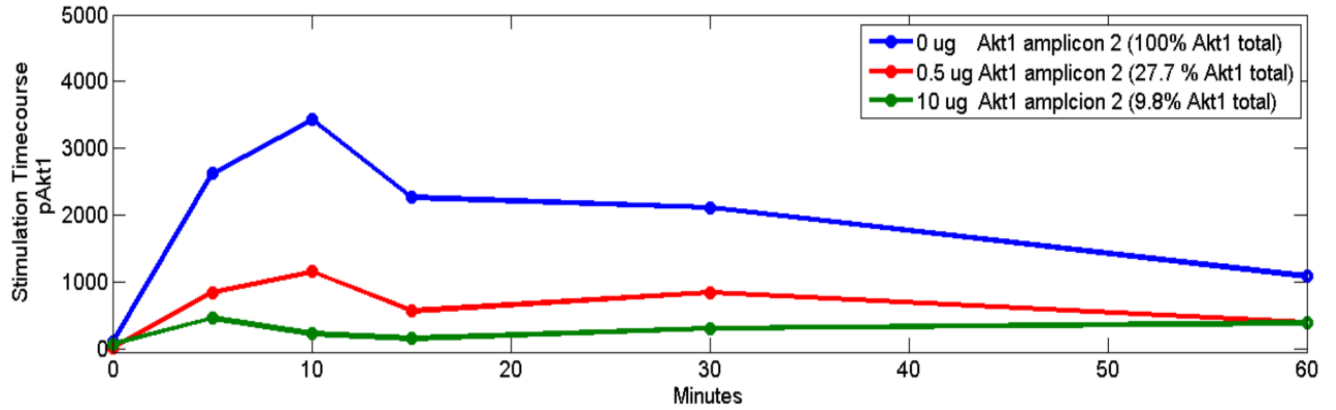


Figure S2 (Related to Figure 2): ROC plot showing the performance of SAINT score based on PRS and RRS. (A) Assessment of baseline network using literature curated PRS and corresponding size controlled RRS. (B) and (C) corresponds to 10 min and 30 min network respectively, PRS and RRS are same as (A). (D-F) Same as (A-C) but the PRS is based on previously published PPIs (including the ones from high-throughput screens) that are supported by 3 or more evidences (see Experimental Procedures).

A



B

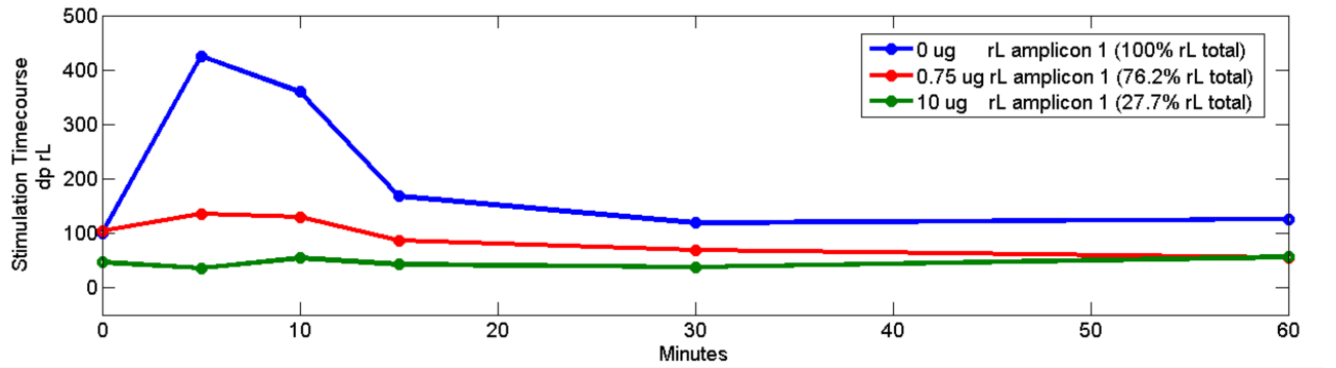


Figure S3 (Related to Figure 3): Plot showing the effect of knocking down of Akt and ERK in the functional RNAi screen. **(A)** RNAi knockdown of Akt reduces the levels of Insulin-induced pAkt. **(B)** RNAi knockdown of ERK reduces the levels of Insulin-induced pERK

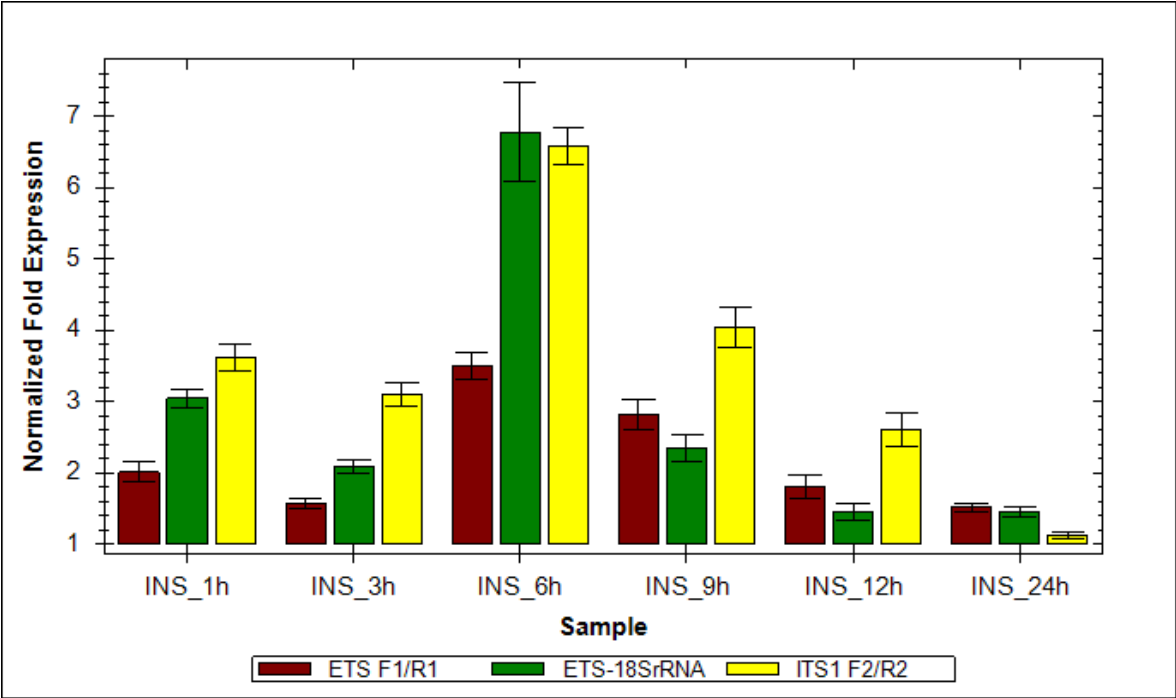


Figure S4 (Related to Figure 7): Characterizing the role of insulin signaling in ribosome biogenesis. Fold-change calculated by normalizing the expression value by baseline condition.

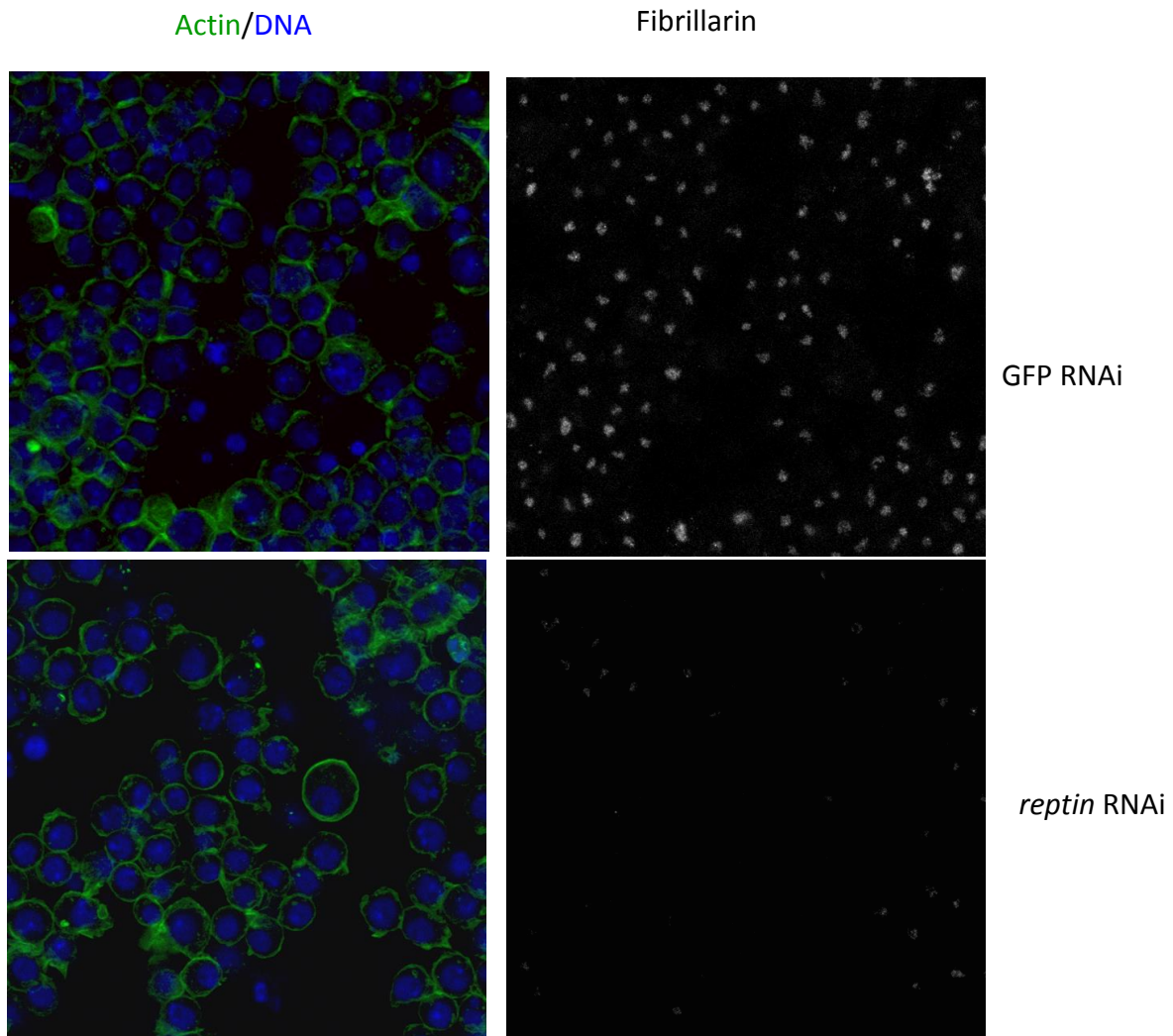


Figure S5 (Related to Figure 7): Characterizing the role of reptin in nucleolar morphology in S2R+ cells. Similar but weaker effects are seen with pontin RNAi in S2R+ cells (data not shown). See also (Demontis and Perrimon, 2009).

References

- Boyle, E.I., Weng, S., Gollub, J., Jin, H., Botstein, D., Cherry, J.M., and Sherlock, G. (2004). GO::TermFinder--open source software for accessing Gene Ontology information and finding significantly enriched Gene Ontology terms associated with a list of genes. *Bioinformatics* 20, 3710-3715.
- Chou, M.F., and Schwartz, D. (2011). Biological sequence motif discovery using motif-x. *Curr Protoc Bioinformatics Chapter 13*, Unit 13 15-24.
- Demontis, F., and Perrimon, N. (2009). Integration of Insulin receptor/Foxo signaling and dMyc activity during muscle growth regulates body size in *Drosophila*. *Development* 136, 983-993.
- Friedman, A., and Perrimon, N. (2006). A functional RNAi screen for regulators of receptor tyrosine kinase and ERK signalling. *Nature* 444, 230-234.
- Friedman, A.A., Tucker, G., Singh, R., Yan, D., Vinayagam, A., Hu, Y., Binari, R., Hong, P., Sun, X., Porto, M., *et al.* (2011). Proteomic and functional genomic landscape of receptor tyrosine kinase and ras to extracellular signal-regulated kinase signaling. *Sci Signal* 4, rs10.
- Hu, Y., Flockhart, I., Vinayagam, A., Bergwitz, C., Berger, B., Perrimon, N., and Mohr, S.E. (2011). An integrative approach to ortholog prediction for disease-focused and other functional studies. *BMC Bioinformatics* 12, 357.
- Kerrien, S., Aranda, B., Breuza, L., Bridge, A., Broackes-Carter, F., Chen, C., Duesbury, M., Dumousseau, M., Feuermann, M., Hinz, U., *et al.* (2012). The IntAct molecular interaction database in 2012. *Nucleic Acids Res* 40, D841-846.
- Keshava Prasad, T.S., Goel, R., Kandasamy, K., Keerthikumar, S., Kumar, S., Mathivanan, S., Telikicherla, D., Raju, R., Shafreen, B., Venugopal, A., *et al.* (2009). Human Protein Reference Database--2009 update. *Nucleic Acids Res* 37, D767-772.
- Kockel, L., Kerr, K.S., Melnick, M., Bruckner, K., Hebrok, M., and Perrimon, N. (2010). Dynamic switch of negative feedback regulation in *Drosophila* Akt-TOR signaling. *PLoS Genet* 6, e1000990.
- Kwon, Y., Vinayagam, A., Sun, X., Dephoure, N., Gygi, S.P., Hong, P., and Perrimon, N. (2013). The Hippo signaling pathway interactome. *Science* 342, 737-740.
- Licata, L., Briganti, L., Peluso, D., Perfetto, L., Iannuccelli, M., Galeota, E., Sacco, F., Palma, A., Nardoza, A.P., Santonico, E., *et al.* (2012). MINT, the molecular interaction database: 2012 update. *Nucleic Acids Res* 40, D857-861.
- Lopes, C.T., Franz, M., Kazi, F., Donaldson, S.L., Morris, Q., and Bader, G.D. (2010). Cytoscape Web: an interactive web-based network browser. *Bioinformatics* 26, 2347-2348.
- Miller, M.L., Jensen, L.J., Diella, F., Jorgensen, C., Tinti, M., Li, L., Hsiung, M., Parker, S.A., Bordeaux, J., Sicheritz-Ponten, T., *et al.* (2008). Linear motif atlas for phosphorylation-dependent signaling. *Sci Signal* 1, ra2.
- Murali, T., Pacifico, S., Yu, J., Guest, S., Roberts, G.G., 3rd, and Finley, R.L., Jr. (2011). Droid 2011: a comprehensive, integrated resource for protein, transcription factor, RNA and gene interactions for *Drosophila*. *Nucleic Acids Res* 39, D736-743.
- Salwinski, L., Miller, C.S., Smith, A.J., Pettit, F.K., Bowie, J.U., and Eisenberg, D. (2004). The Database of Interacting Proteins: 2004 update. *Nucleic Acids Res* 32, D449-451.
- Shannon, P., Markiel, A., Ozier, O., Baliga, N.S., Wang, J.T., Ramage, D., Amin, N., Schwikowski, B., and Ideker, T. (2003). Cytoscape: a software environment for integrated models of biomolecular interaction networks. *Genome Res* 13, 2498-2504.
- Sopko, R., Foos, M., Vinayagam, A., Zhai, B., Binari, R., Hu, Y., Randklev, S., Perkins, L.A., Gygi, S.P., and Perrimon, N. (2014). Combining genetic perturbations and proteomics to examine kinase-phosphatase networks in *Drosophila* embryos. *Dev Cell* 31, 114-127.

Stark, C., Breitkreutz, B.J., Chatr-Aryamontri, A., Boucher, L., Oughtred, R., Livstone, M.S., Nixon, J., Van Auken, K., Wang, X., Shi, X., *et al.* (2011). The BioGRID Interaction Database: 2011 update. *Nucleic Acids Res* 39, D698-704.

Vinayagam, A., Hu, Y., Kulkarni, M., Roesel, C., Sopko, R., Mohr, S.E., and Perrimon, N. (2013). Protein complex-based analysis framework for high-throughput data sets. *Sci Signal* 6, rs5.

Yellaboina, S., Tasneem, A., Zaykin, D.V., Raghavachari, B., and Jothi, R. (2011). DOMINE: a comprehensive collection of known and predicted domain-domain interactions. *Nucleic Acids Res* 39, D730-735.